Colloid Polym Sci 274:73–80 (1996)

SHORT COMMUNICATION

T. Okubo
H. Fujita
K. Kiriyama
H. Yamaoka

Colloidal single crystals of silica spheres in the presence of simple- and poly-electrolytes, and ionic detergents

Received: 7 June 1995
Accepted: 8 August 1995

Prof. Dr. T. Okubo[1] (✉) · H. Fujita
K. Kiriyama · H. Yamaoka
Department of Polymer Chemistry
Faculty of Enginnering
Kyoto University
Kyoto 606-01, Japan

[1] Current address:
Department of Applied Chemistry
Faculty of Engineering
Gifu University, Gifu 501-11, Japan

Abstract Colloidal single crystals of silica spheres (103 nm in diameter) are formed in the presence of various kinds of salts 1 simple electrolytes, i.e., sodium chloride, calcium chloride and lanthanum chloride, 2 polyelectrolytes such as 3–6 type ionen polymer (polybrene), poly-*N*-ethylpyridinium bromide, a copolymer of *N*-benzyl pyridinium chloride and *N*-hexadecyl pyridinium bromide, and sodium polyethylene sulfonate, and 3 cationic and anionic detergents, hexadecyltrimethylammonium bromide and sodium dodecylsulfate. Shape and size of their single crystals, phase diagram, and the relationship between the two parameters among the critical concentration of melting, conductance and pH of the crystal-like suspensions have been studied. Colloidal single crystals of *positively charged spheres* have been formed in this study by the method of the charge reversal of spheres through the strong adsorption of cationic polyelectrolytes onto the anionic silica spheres.

Key words Colloidal crystals – silica spheres – electrical double layer – single crystals

Introduction

Glittering and brilliant colors of the colloidal single crystals observed with the naked eye in suspension are quite beautiful and exciting. A study of colloidal crystals is helpful in understanding the fundamental characters of crystallization of matters, phase equilibria and electrostatic interactions of macroionic systems [1–15]. Quite recently, very large size of single crystals have been formed for the exhaustively deionized and very diluted aqueous suspensions and alcoholic organic solvents [16–19]. Two essentially important factors causing the colloidal crystals are an electrostatic intersphere repulsion and an expanded electrical double layers around the spheres in the deionized state. Thus, it will be easily expected that the critical concentration of melting increases by the addition of the salts, since the thickness of the electrical double layers decreases sharply as the ionic concentration of the suspension increases. Main purpose of this work is to obtain the reliable data on the *phase diagrams* of colloidal crystallization in the presence of various kinds of salts, and to support the importance of the electrical double layers for the crystal-like structure formation. As is well known, most colloidal spheres in aqueous media are negatively charged except artificial modification of sphere surfaces, and colloidal crystals of the combination of cationic spheres and anionic double layers have not been reported hitherto. Thus, the second purpose of this work is to investigate the colloidal single crystals of *positively charged spheres* by the technique of the charge reversal of the sphere surface by the strong adsorption of cationic polyelectrolytes onto the surface of anionic silica spheres.

CPS 612

Colloid & Polymer Science, Vol. 274, No. 1 (1996)

Experimental

Materials

Colloidal silica spheres of CS-81 in aqueous suspension was a gift from Catalyst & Chemicals Ind. Co. (Tokyo). Diameter (d), standard deviation (δ) from the mean diameter, and polydispersity index (δ/d) were 103 nm, 13.2 nm, and 0.13, respectively. The values of d and δ were determined from an electron microscope (EM400-T, Philips Co.) equipped with an image micro-processor by courtesy of Dr. S. Aotani of Synthetic Rubber Co. (Tokyo). The charge density of the spheres was determined by conductometric titration with a conductivity meter, model DS-14 (Horiba Co., Kyoto). Charge density of strongly acidic groups was 0.38 $\mu C/cm^2$, where sphere surface was assumed to be rigid and smooth. The sphere sample was carefully purified several times using an ultrafiltration cell (model 202, membrane: Diaflo-XM300, Amicon Co.). Then the sample was treated on a mixed bed of cation- and anion-exchange resins [Bio-Rad, AG501-8(D), 20–50 mesh] for at least 1 month. Water used for the purification and for suspension preparation was deionized by using cation- and anion-exchange resins [Puric-R, type G10, Organo Co. (Tokyo)], purified by a Milli-Q reagent grade system (Millipore Co., Bedford, MA), and further treated with the ion-exchange resins of Bio-Rad.

Sodium chloride, calcium chloride, sodium sulfate, and lanthanum chloride were the purest grade reagents available commercially in our laboratory. Sodium poly(ethylene sulfonate) (NaPES) was purchased from Polyscience Inc. (Warrington, PA). Aqueous solution of NaPES was passed through a column of a mixed bed of cation- and anion-exchange resins (Bio-Rad) repeatedly in acid form. Sodium salt was obtained by neutralization of the acid with sodium hydroxide solution. The 3–6 ionen type cationic polymer, Polybrene (PB), 1,5-dimethyl-1,5-diazaundicamethylene polymethobromide, was purchased from the Aldrich Chemical Co. (Milwaukee, WI). The details on the preparation and purification of poly-4-vinyl-*N*-ethylpyridinium bromide (C2PVP), and copolymer of 4-vinyl-*N*-benzylpyridinium chloride (95%) and 4-vinyl-*N*-*n*-hexadecylpyridinium bromide (5%) (C16BzPVP) were described in previous papers [20]. The degree of quaternization was 0.97. The degree of polymerization of poly-4-vinylpyridine (parent polymer) was 3800 by viscometry. Hexadecyltrimethylammonium bromide (CTABr) and sodium dodecylsulfate (SDS) were guaranteed grade reagents purchased from Wako Pure Chemicals (Osaka) and used after further purification by recrystallization from ethanol and refluxing in *n*-hexanol.

Close-up and microscopic photographing

Phase diagram (critical concentration of melting) between the crystal-like and liquid-like structures were obtained clearly from the direct observation with the naked eyes. Colloidal suspensions were prepared in the test tubes (disposable culture tube, borosilicate glass, Corning Glass Works, Corning, NY, 11 and 13 mm, inside and outside diameters) shielded with Parafilm (American Can Co., Greenwich, CT) tightly. Photographing of colloidal crystals was made with a Canon EOS10 camera, macro-lens (EF50 mm, $f = 2.5$) and life-size converter EF. Velvia film (Fujichrome, RVP135, ISO = 50) was used. Light source was a pocket-type flash light (Xenon type, BF-775, National). Microscopic color photographs were taken with a reversed-type metallurgical microscope, type PME3 (Olympus, Tokyo). The single crystals were observable through the bottom and side walls of the test tube cells with an objective lens, Neo D Plan (5× or 10×).

ζ-Potential, conductance, and pH measurements

ζ-Potential measurements were made with an electrophoretic light scattering spectrophotometer, type ELS-800 (Otsuka Electronics, Osaka). Conductance and pH of the crystal-like suspensions were measured on a Horiba conductivity meter, model DS-14 (Kyoto) with a Horiba electrode, type 3552 (cell constant is 1.028), and Beckman pH meter ϕ-34 (Fullerton, CA), respectively.

Results and discussion

Shape and size of the single crystals in the presence of salts

Figure 1 shows the microscopic color photographs of the colloidal single crystals from the homogeneous nucleation mechanism in the aqueous bulk phase of suspensions in the presence of sodium chloride. In this experiment 2×10^{-5} mol/L of NaCl was added and the sphere concentration was also rather high, $\phi = 0.0360$. Size of single crystals was smaller than 1 mm, and shape of the crystals was observed with a microscope. Difference in colors between (a) and (b) are due to the difference in the angles of the incident light and/or the direction of observation against the Bragg planes. Color was the same throughout the same crystals, and then each crystal is undoubtedly single crystals as a whole. Interestingly, separation of the single crystals into the flakes was observed especially when the sample tubes left to stand on desk more than ten hours. This may be due to the faint shearing forces upon the test tubes from the very weak mechanical vibration of the desk,

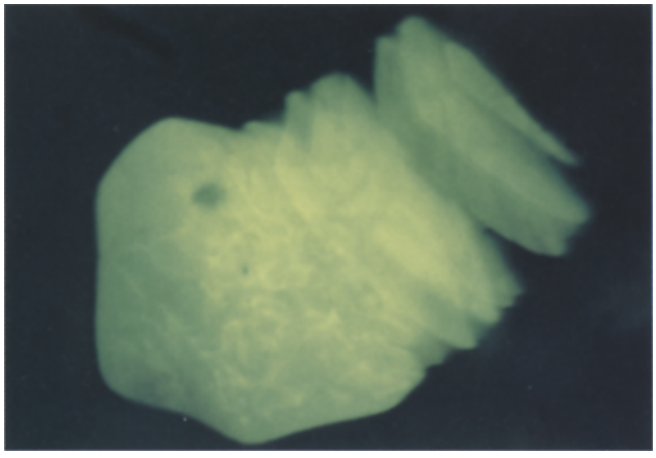

(a)

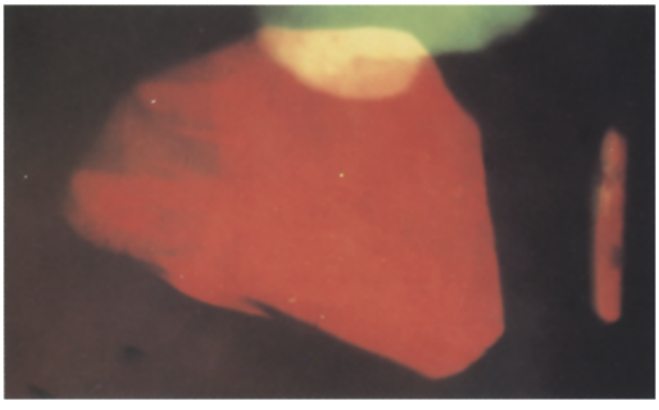

(b)

Fig. 1 Microscopic observation of colloidal single crystals of CS-81 spheres in the presence of NaCl at 25 °C. $\phi = 0.0360$, [NaCl] = 2.00×10^{-5} mol/L. Frame size = (a) 1.2 mm × 1.76 mm, (b) 0.82 mm × 1.2 mm

though the exact reason is not clear yet. The single crystals in Fig. 1 were block-like and were crystallized from the homogeneous nucleation mechanism in the bulk phase far from the cell wall [16–19]. It should be noted here that these single crystals were melted away quite easily into the super-cooled liquid-like structures, when the suspension was mixed invertedly. However, the crystallization occurred again when the test tube left to stand. This kind of melting and crystallization processes occurred every time when the suspension was mixed. However, shape of the single crystals formed differed greatly. Size of the single crystals formed also differed largely for each experiment.

Figures 2(a) and (b) are close-up color pictures of single crystals grown up in the salt containing suspensions, NaCl and PB, respectively. Width of the picture corresponds to the outside diameter of the test tube of 13 mm. All the block-like crystals are those from the homogeneous nucleation mechanism. Change in colors from yellowish to reddish in the single crystal seen in the bottom region of the test tube in Fig. 2(a) is due to the change in the incident angles of light through the curved cell wall. The small red spots, which are located along the test tube in the right-hand side of the picture 2(a), show the single crystals grown up perpendicularly to the cell wall from the heterogeneous nucleation mechanism along the inner surfaces of the test tube. Clearly, the salt-containing suspensions of colloidal crystals were much turbid compared with the salt-free and/or deionized suspensions [16–18]. When the suspension is turbid, only the single crystals close to the cell wall are observable with the naked eye. The reason why color of these single crystals were monochromatic will be the fact that the single crystals from the homogeneous nucleation close to the cell wall are apt to be oriented keeping the (111) planes of the crystal parallel to the cell wall [18].

Figure 3 shows the microscopic observation of colloidal crystals of CS-81 spheres from the homogeneous nucleation mechanism in the presence of the various amounts of NaPES, anionic polyelectrolyte. Shape of the single crystals was quite similar to that of NaCl or PB containing suspensions shown in Fig. 1. Separation into flakes was observed again. The slipping planes of the flakes would be (111) lattice planes of the fcc crystal structure.

Phase diagram

Figure 4 shows the phase diagram between crystal-like and liquid-like structures in the presence of sodium chloride. Five different sizes of open circles in the figures indicate the round size of the single crystals which appeared, i.e., smaller than 0.1 mm (shown by the smallest open circles in the figures), 0.1 to 0.5 mm (secondary small open circles), 0.5 to 1.5 mm (medium size), 1.5 to 2.5 mm (secondary large open circles) and larger than 2.5 mm (largest open circles), respectively. In this figure the ϕ values with and without ion-exchange resins were given at 2×10^{-7} mol/L and 1×10^{-6} mol/L of sodium chloride, respectively. Clearly, the critical sphere concentration of melting, ϕ_c increased substantially by the addition of a small amount of sodium chloride. Furthermore, it is interesting to note in the figure that rather large single crystals were formed even in the presence of large amount of sodium chloride close to 10^{-4} mol/L.

According to the effective hard-sphere model [21–27], colloidal crystal is formed when the effective diameter (d_{eff}) of the colloidal spheres, which includes the Debye

Colloid & Polymer Science, Vol. 274, No. 1 (1996)

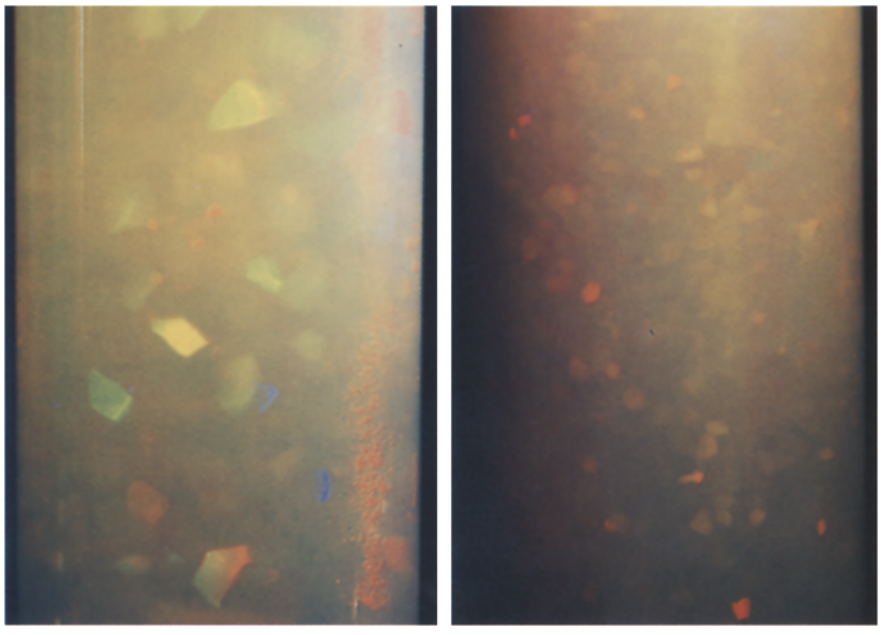

Fig. 2 Close-up color photographs of CS-81 spheres in the presence of NaCl (a) and PB (b) at 25 °C. Width of the picture = 11 mm, (a) $\phi = 0.0120$, [NaCl] = 2.86×10^{-6} mol/L, 7 min after vertical mixing, exposure = 2 s, iris = 22, (b) $\phi = 0.0360$, [PB] = 1.71×10^{-5} equiv/L, 12 min after virtical mixing, exposure = 0.7 s, iris = 27

screening length (D_l), is close to or larger than the observed intersphere distance (D), i.e., d_{eff} [$= 2 \times D_l +$ diameter (d)] $\geq D$. In crystal-like structures, the spheres fluctuate around their equilibrium points. When d_{eff} is comparable to or a bit shorter than the D value, the distribution of the spheres is usually liquid-like, and the spheres move without keeping their positions. When d_{eff} is much shorter than D, a gas-like distribution is observed. Note here that the observed intersphere spacing (D) was always close to the calculated mean intersphere distance (D_o). The Debye-screening length, D_l is given by Eq. (1).

$$D_l = (4\pi e^2 n/\varepsilon k_B T)^{-1/2}, \quad (1)$$

where e is the electronic charge, ε is the dielectric constant of the solvent, k_B is the Boltzmann constant and n is the concentration of free-state cations and anions in suspension, and given by $n = n_c + n_s + n_o$, where n_c is the concentration (number of ions per cm^3) of diffusible counterions, n_s is the concentration of foreign salt, sodium chloride, for example. n_o is the concentration of both H^+ and OH^- from the dissociation of water. In order to estimate n_c, the fraction of free-state counterions (β) must be known. Note that the maximum value of D_l observed hitherto was ca. 1 μm in water. The similar value of D_l, i.e., 1.0 μm, is also estimated from Eq. (1) by taking $n_o = 2 \times 10^{-7}$ (mol/dm^3) $\times$ $N_A \times 10^{-3}$ cm^{-3}, where N_A is Avogadro's number. It should be mentioned here that β-values are very small for typical colloidal particles [2, 28–30].

Table 1 compares the D_l values calculated and observed in NaCl-containing suspensions. The observed values of the Debye-screening length, $D_{l,obs}$ are given by Eq. (2),

$$D_{l,obs} = (D_c - d)/2, \quad (2)$$

where D_c is the intersphere distance calculated at the critical sphere concentration of melting, ϕ_c. c_c in the table indicates the critical salt concentration of melting, and n^* is the total concentration of diffusible simple ions given by the unit of mol/L. Here, β was assumed to be 0.1 irrespective of the ionic concentration of the suspension, though β is expected to decrease slightly with increasing concentration of NaCl [28]. Clearly, for the salt-free suspensions, the calculated values of the Debye-length agreed with or larger than the observation, which supports strongly the validity of the effective hard sphere model for the salt-free systems with and without ion-exchange resins.

For the NaCl-containing systems the calculated D_l value was smaller than the observed one. This means, for the first glance, that the suspensions are liquid-like instead of crystal-like. However, it will be recalled that the adsorption of sodium chloride onto the surface of the colloidal spheres is influential as will be discussed later in detail. $D_{l,calc}$ values are clearly underestimated for the NaCl-containing suspensions by the adsorption effect. Thus, the agreement of $D_{l,calc}$ with $D_{l,obs}$ will be good, when the adsorption effect of sodium chloride on colloidal sphere is taken into account.

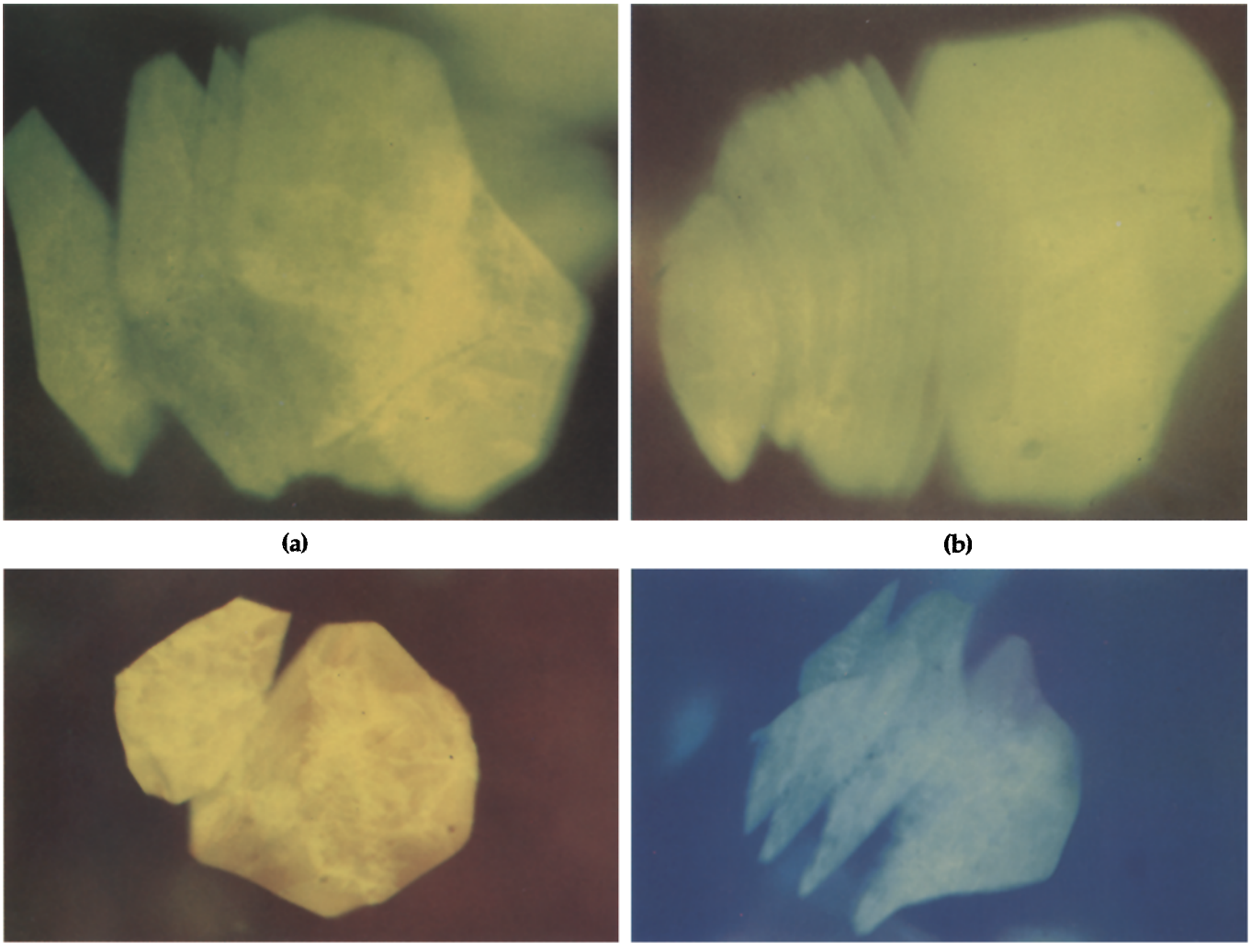

Fig. 3 Microscopic observation of colloidal single crystals of CS-81 spheres in the presence of NaPES at 25 °C. $\phi = 0.0360$, (a) [NaPES] = 1.36×10^{-5} equiv/L, (b) 1.70×10^{-5} equiv/L, (c) 2.40×10^{-5} equiv/L, (d) 2.38×10^{-5} equiv/L. Frame size = 1.2 mm × 1.76 mm

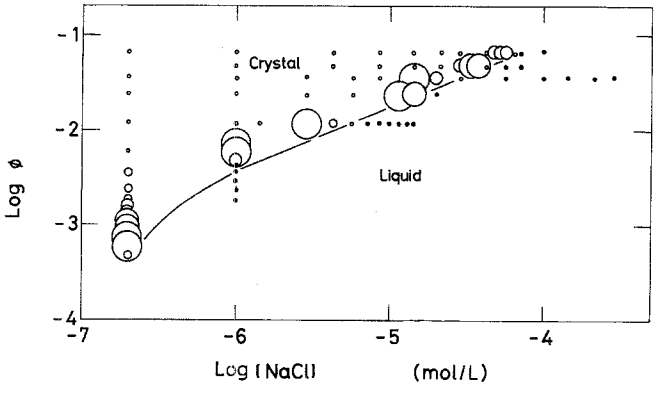

Fig. 4 Phase diagram of colloidal crystals of CS-81 spheres in the presence of NaCl at 25 °C. Open and solid circles show the crystal-like and liquid-like structures

Table 1 Parameters in the effective hard-sphere model for NaCl-containing suspension

ϕ_c	c_c (mol/L)	n^* (equiv/L)	$D_{l,calc}$ (nm)	$D_{l,obs}$ (nm)
0.00045[a]	0[a]	3×10^{-7}	780	560
0.004	0	2.1×10^{-6}	300	240
0.012	5.8×10^{-6}	1.4×10^{-5}	115	150
0.024	1.6×10^{-5}	3.7×10^{-5}	70	110
0.036	2.9×10^{-5}	6.6×10^{-5}	53	90
0.048	4.0×10^{-5}	9.1×10^{-5}	45	77
0.066	6.5×10^{-5}	1.45×10^{-4}	36	64

[a] Deionized suspension, taken from ref. [18].

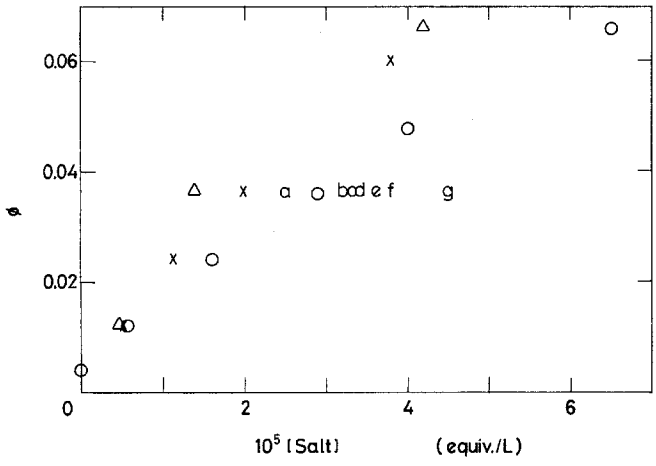

Fig. 5 Phase diagram of colloidal crystals of CS-81 spheres in the presence of NaCl(O), $CaCl_2$(X), $LaCl_3$(Δ), PB(a), C2PVP(b), C16BzPVP(c), CTABr(d), Na_2SO_4(e), and SDS(g) at 25 °C

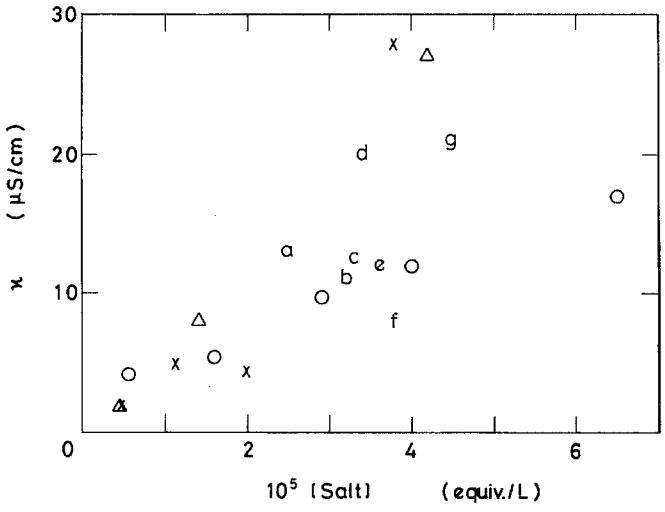

Fig. 6 Specific conductance of the critical suspension of melting for colloidal crystals of CS-81 spheres in the presence of NaCl(O), $CaCl_2$(X), $LaCl_3$(Δ), PB(a), C2PVP(b), C16BzPVP(c), CTABr(d), Na_2SO_4(e), NAPES(f), and SDS(g) at 25 °C

Phase diagram in the presence of various kinds of salts is shown in Fig. 5. Clearly, the critical *salt* concentrations of melting at the same ϕ_c value were in the order,

$$LaCl_3 < CaCl_2 < PB < NaCl < C2PVP \leq C16BzPVP \leq CTABr < Na_2SO_4 < NaPES < SDS. \quad (3)$$

It should be noted that the order of the critical *sphere* concentration is just opposite order to Eq. (3). The order (3) teach us that the colloidal crystals are broken effectively by the addition of $LaCl_3$, and SDS is weakest in the melting action. Thus, the order (3) shows clearly that the order of the melting power is following.

$$\text{Simple-cations} < \text{Poly-cations} < \text{Simple-anions} < \text{Poly-anions}. \quad (4)$$

When the simple-cations such as $LaCl_3$ and $CaCl_2$ are added into the crystal-like suspension, the release of the hydronium ions, which are originally fixed (bound) to the colloidal anionic charges by the counter-ion binding effect, occurs and results in the increase in the ionic concentration of the suspension and also results in the melting of the crystals by the thinning of the electrical double layers. As will be discussed later section, the release of the hydronium ions induced by the addition of $LaCl_3$ and $CaCl_2$ was supported strongly by the several experimental results in this work, i.e., increase in the conductance demonstrated in Fig. 6, decrease in pH in Fig. 7, and linear relationship of $\log\kappa$ with pH with a slope of minus unity in Fig. 8. It should be mentioned here that the reversal of the sign of the sphere charge from minus to plus may not occur when $LaCl_3$ or $CaCl_2$ are added. This is consistent with the fact that the ζ-potential increased from −53 mV to −20 mV

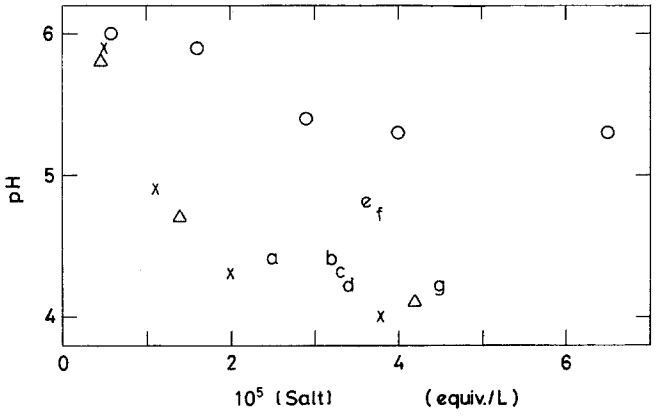

Fig. 7 pH values of the critical suspension of melting for colloidal crystals of CS-81 spheres in the presence of NaCl(O), $CaCl_2$(X), $LaCl_3$(Δ), PB(a), C2PVP(b), C16BzPVP(c), CTABr(d), Na_2SO_4(e), NAPES(f), and SDS(g) at 25 °C

but the charge reversal did not occur as is seen in Table 2 [31]. Here, the values of the zeta potential shown in the second row of Table 2 were observed by the electrophoretic light scattering measurements for the suspensions, in which the sample suspensions were diluted with the hundred-fold amount of water. The zeta potential of the sample suspensions themselves were not measured, since the sphere concentrations were too high for the measurements. The ζ-potentials of the sample suspensions are, therefore, estimated to be much larger than the observation. The zeta-potential values given in the fourth row of the table were taken from our previous work for the aqueous suspensions containing a tiny amount of colloidal

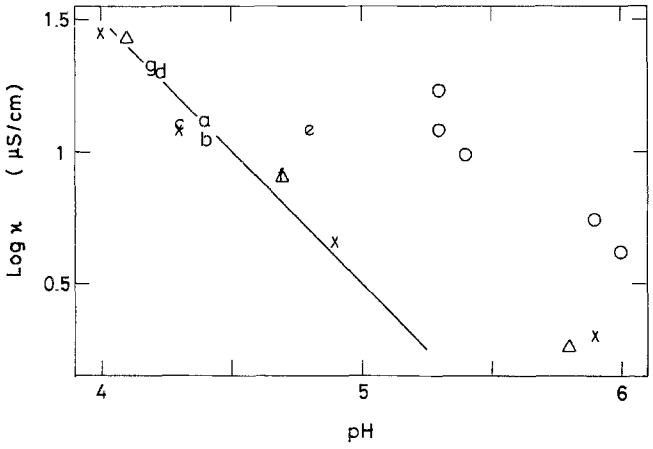

Fig. 8 Relationship between log κ and pH in the critical suspension of melting for colloidal crystals in the presence of NaCl(O), $CaCl_2$(X), $LaCl_3$(Δ), PB(a), C2PVP(b), C16BzPVP(c), CTABr(d), Na_2SO_4(e), NAPES(f), and SDS(g) at 25 °C

Table 2 Zeta-potential of diluted suspensions of silica spheres in the presence of salts

Salt	ζ-potential (mV)	[salt][a](equiv/L)	ζ-potential (mV)[a]
none	-49 ± 2	0	-53 ± 0.5
NaCl	–	2×10^{-6} to 6×10^{-4}	-54 ± 1
$CaCl_2$	–	2×10^{-5} to 8×10^{-4}	-32 ± 2
$LaCl_3$	$-47 + 2$	6×10^{-5} to 1.2×10^{-3}	-20 ± 1
PB	-43 ± 4	1×10^{-7} to 3×10^{-4}	$+15$ to $+64$
C2PVP	$+4 \pm 1$	2×10^{-7} to 3×10^{-4}	$+10$ to $+60$
C16BzPVP	-35 ± 3	1×10^{-7} to 3×10^{-4}	$+5$ to $+62$
Na_2SO_4	-60 ± 8	4×10^{-5} to 4×10^{-4}	-56 ± 3
NaPES	-59 ± 4	5×10^{-6} to 1×10^{-4}	-72 ± 3

[a] Taken from ref. [31].

silica spheres and the salts of the concentrations given in third row.

The release of hydronium ions by the addition of the poly-cations (PB, C2PVP, C16BzPVP and CTABr) is also supported by the increase in conductance (shown in Fig. 6) and also by the linear relationship between logκ and pH (in Fig. 8). However, most significant effect was the *charge reversal* from negative to positive (see, Table 2). Furthermore, the reversal effect was in the order PB > C2PVP > C16BzPVP, which tells us that the strongly hydrophobic polymers are adsorbed weakly on the surfaces of the colloidal silica spheres. This supports the notion that the hydrophobicity of the silica spheres is very weak. Instead of the hydrophobic interactions the dipole–dipole forces between silanol groups of silica surfaces and the poly-cations [31] will be effective. Furthermore, the order in the strength of the reversal effect among the poly-cations supports that the adsorption of the bulky poly-cations is not so easy by the stereo-chemical effects [31]. Formation of the colloidal crystals of the positively charged colloidal spheres is highly interesting. These systems have not been reported hitherto as the authors are aware of.

The critical salt concentrations of the suspensions containing SDS, NaPES and Na_2SO_4 were high. This will be due to the fact that these poly-anions do not interact specifically with the anionic colloidal particles so strongly.

Specific conductance and pH of the critical suspensions of melting

In order to examine the ionic nature of the suspensions of colloidal crystals, specific conductance (κ) and pH values were measured for the critical suspensions of melting. Figure 6 shows the κ values. Clearly, the values for the suspensions containing $LaCl_3$ and $CaCl_2$ were high compared with others. This is safely ascribed to the release of the hydronium ions by the polyvalent simple-cations. More than ninety percent of the sphere charges and their counter-ions (hydronium ions in most cases) are bound by the electrostatic attractive forces between the sphere's negative charges and the positive counter-ions [2, 28–30]. However, release of the hydronium ions also occurs by the strong adsorption of La^{3+} or Ca^{2+} onto the sphere surfaces as,

$$H_{3n}(\text{Sphere}) + nLa^{3+} \rightarrow La_n(\text{Sphere}) + 3n\,H^+ . \quad (5)$$

Figure 7 shows the pH values of the critical suspensions of melting. By the addition of $LaCl_3$ and/or $CaCl_2$, substantial decrease in pH values was observed, which is also explained with the release of the hydronium ions by the binding of the multi-valent cations on to the sphere surfaces. Figure 7 also supports that the release of the hydronium ions by the poly-cations such as PB, C2PVP, C16BzPVP and CTABr is significant. It is interesting to note that the addition of the poly-anions caused the decrease in pH values. This may support that the adsorption effect of the polyanions is not neglected. As is clear in the figure, weak adsorption of sodium chloride on to the spheres is suggested from the slight decrease in pH by the addition of sodium chloride.

Figure 8 shows the relationship between the logarithum of the specific conductance of the critical suspensions of melting and the pH values of the same suspensions. Interestingly, the linear relationship was observed with a slope of minus unity especially at high values of these parameters except the suspensions containing NaCl and Na_2SO_4. This relationship supports that the main contribution for the suspension conductance is ascribed to that of hydronium ions. Rowell et al. [32, 33] have developed

a new technique of the fingerprinting, which was effective to clarify the ionic character of colloidal spheres. In this technique, several kinds of experimental parameters such as electrophoretic mobility, conductance and pH were measured for the same suspension, and the relationship among the parameters was analysed. Figure 8 in this work will be one of the simple examples of the fingerprinting techniques.

Acknowledgements This work was supported by grants-in-aid from Nissan Science Foundation. Catalyst & Chemicals Ind. Co. and Otsuka Electronics Co. (Osaka) are sincerely acknowledged for the kind offer of silica sphere sample and for the kind help in the electrophoretic light-scattering measurements, respectively. Dr. S. Aotani of Synthetic Rubber Co. (Tokyo) is also acknowledged sincerely for his kind help on the measurements of the electron microscopy.

References

1. Luck W, Klier M, Wesslau H (1963) Ber Bunsenges Phys Chem 67:75, 84
2. Vanderhoff W, van de Hul HJ, Tausk RJM, Overbeek JThG (1970) In: Goldfinger G (ed) Clean Surfaces: Their Preparation and Characterization for Interfacial Studies. Dekker, New York
3. Hiltner PA, Papir YS, Krieger IM (1971) J Phys Chem 75:1881
4. Kose A, Ozaki M, Takano K, Kobayashi Y, Hachisu S (1973) J Colloid Interface Sci 44:330
5. Crandall RS, Williams R (1977) Science 198:293
6. Mitaku S, Otsuki T, Okano K (1978) Jpn J Appl Phys 17:305
7. Clark NA, Hurd AJ, Ackerson BJ (1979) Nature 281:57
8. Lindsay HM, Chaikin PM (1982) J Chem Phys 76:3774
9. Tomita M, Takano K, van de Ven TGM (1983) J Colloid Interface Sci 92:367
10. Pieranski P (1983) Contemp Phys 24:25
11. Pusey PN, van Megen W (1986) Nature 320:340
12. Okubo T (1988) Acc Chem Res 21:281
13. Ottewill RH (1989) Langmuir 5:4
14. Russel WB, Saville DA, Schowalter WR (1989) In: Colloidal Dispersions. Cambridge University Press, Cambridge
15. Okubo T (1993) Prog Polymer Sci 18: 481
16. Okubo T (1992) Naturwissenschaften 79:317
17. Okubo T (1993) Colloid Polym Sci 96:61
18. Okubo T (1994) Langmuir 10:1695
19. Okubo T (1994) Langmuir 10:3529
20. Ishiwatari T, Okubo T (1980) J Polymer Sci 18:1807
21. Baker JA, Henderson D (1967) J Chem Phys 47:2856
22. Wadachi M, Toda M (1972) J Phys Soc Jap 32:1147
23. Hachisu S, Kobayashi Y, Kose A (1973) J Colloid Interface Sci 42:342
24. Brenner SL (1976) J Phys Chem 80:1473
25. Takano K, Hachisu S (1977) J Chem Phys 67:2604
26. Barnes CJ, Chan DY, Everett DH, Yates DE (1978) J Chem Soc Faraday Trans 2 74:136
27. Voeglli LP, Zukoski IV CF (1991) J Colloid Interface Sci 141:79
28. Okubo T (1987) Ber Bunsen-ges Phys Chem 91:1064
29. Alexander S, Chaikin PM, Grant P, Morales GJ, Pincus P, Hone D (1984) J Chem Phys 80:5776
30. Okubo T (1988) J Colloid Interface Sci 125:380
31. Okubo T (1990) Polymer Bull 23:211
32. Rowell RL, Shiau SJ, Marlow BJ (1991) In: Provder T (ed) Particle Distribution II. Assessment and Characterization. ACS Symposium Series 472, American Chemical Society, Washington DC
33. Prescott JH, Shiau S, Rowell RL (1993) Langmuir 9:2071